Polymer 50 (2009) 1351–1357

Contents lists available at ScienceDirect

Polymer

journal homepage: www.elsevier.com/locate/polymer

In situ mid-IR and UV–visible spectroscopies applied to the determination of kinetic parameters in the anionic copolymerization of styrene and isoprene

Sébastien Quinebèche [a], Christophe Navarro [b], Yves Gnanou [a,*], Michel Fontanille [a,*]

[a] *Laboratoire de Chimie des Polymères Organiques, Université Bordeaux-1/ENSCPB/CNRS, 16, Av. Pey-Berland, 33607 PESSAC, France*
[b] *Arkema France, Groupement de Recherches de Lacq, 64170, LACQ, France*

ARTICLE INFO

Article history:
Received 8 December 2008
Received in revised form
15 January 2009
Accepted 16 January 2009
Available online 24 January 2009

Keywords:
Anionic copolymerization
Kinetics of polymerization
In situ infrared and UV–visible spectroscopies

ABSTRACT

In situ MIR and UV–visible spectroscopies have been combined in a set-up that has been used to monitor anionic (co)polymerizations of styrene and isoprene. This experimental set-up gives access to the simultaneous and real time concentrations of monomers and actives species during the polymerization, through optical fibers probes immersed in the reaction medium. This method allows fast, accurate and reproducible measurements of the rate constants of the (co)polymerizations investigated even if it does not resort to high vacuum. The influence of some experimental factors has been examined using this method. Among the kinetic parameters governing the (co)polymerization of styrene and isoprene initiated by *sec*-butyllithium, the influence of the nature of solvent was investigated. It appears that the only reaction to depend on the nature of the aromatic solvent ($k_{\mathrm{ss,toluene}} > k_{\mathrm{ss,ethylbenzene}}$) is the propagation step of styrene.

1. Introduction

The anionic (co)polymerization of styrene and diene monomers, initiated by alkyllithium, is particularly suitable for the preparation of well-defined (co)polymers with controlled composition, predictable and little disperse molar masses [1–4]. Each polymer chain is grown from a single reactive site and block copolymers result from the sequential addition of monomers. ABC poly(styrene-*b*-butadiene-*b*-methyl methacrylate) triblock terpolymers (SBM), known for their nanostructured properties, are a recent addition in the class of anionically prepared polymers. For an industrial implementation of the anionic synthesis of such a terpolymer, kinetic studies are essential to optimize the polymerization conditions (polymerization time, temperature of reaction, solvent…). In this study, we describe a novel experimental set-up that allows a fast and easy access to kinetic parameters pertaining to (co)polymerizations carried out in the conditions used by industry to anionically prepare the above mentioned materials.

Various techniques, including gas chromatography [5], dilatometry [6], absorption spectroscopies [7–14], have been used in the past to draw kinetic data from anionic polymerization processes. Among absorption spectroscopies, near-infrared [9] (NIR) and Raman [7] spectroscopies are appropriate tools that were successfully applied in kinetic studies of anionic (co)polymerization of styrene and diene monomers. However, it has been shown in this last decade that mid-infrared (MIR) spectroscopy is probably the most convenient technique to monitor living polymerizations. Actually, *in situ* MIR spectroscopy was successfully used in the studies of the cationic (co)polymerization of isobutene and styrene [15–19] and the anionic (co)polymerization of 1,3-cyclohexadiene and styrene [11,12]. An optic fiber probe introduced in the reaction medium enables real time *in situ* MIR measurements of the monomer consumption without the need for sampling out. The collected data give access to kinetic parameters such as the propagation rate constants and the reactivity ratios.

In anionic (co)polymerization of styrene and diene monomers, UV–visible spectroscopy is eminently suitable to measure the concentration in active centers [20]. For that reason, our aim was to combine *in situ* MIR and UV–visible spectroscopies to measure simultaneously the concentrations in monomer(s) and active species in the anionic (co)polymerization of the above mentioned monomers (Fig. 1).

We report herein the determination of homo- and cross-propagation rate constants (k_{ss}, k_{ii}, k_{si} and k_{is}) in the anionic polymerization of styrene and isoprene and their copolymerization in several non-polar solvents, using the association of these two spectroscopic techniques. The same analytic set-up served also to measure the reactivity ratios of the statistical copolymerization of styrene and isoprene (r_{s} and r_{i}) from one single experiment.

---

* Corresponding authors. Tel.: +33 5 40 00 64 23.
E-mail addresses: gnanou@enscpb.fr (Y. Gnanou), fontanille@enscpb.fr (M. Fontanille).

0032-3861/$ – see front matter © 2009 Elsevier Ltd. All rights reserved.
doi:10.1016/j.polymer.2009.01.041

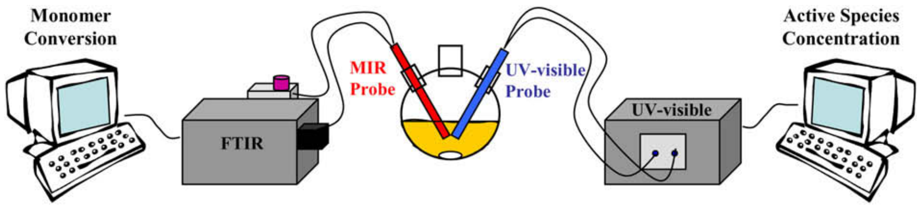

Fig. 1. Real time monitoring of anionic polymerization using a combination of FTIR and UV–visible spectroscopies.

2. Experimental section

2.1. Materials

Cyclohexane, benzene, toluene (99%, J. T. Baker) and ethylbenzene (99%, Aldrich) were first degassed, dried over calcium hydride and distilled. Then, they were purified by mixing with polystyryllithium seeds and distilled prior to use. Styrene and isoprene (99%, Aldrich) were degassed, dried by distillation over calcium hydride and purified before use by distillation over di-*n*-butylmagnesium. All distillations were carried out under reduced pressure. Solvents and reactants were stored under dry argon in glass apparatuses fitted with PTFE stopcocks.

sec-Butyllithium (1.4 M in cyclohexane, Aldrich) was filtered and diluted with pure cyclohexane. The solution was titrated using *N*-pivaloyl-*o*-toluidine [21]. *sec*-Butyllithium was transferred using syringe under argon flow.

2.2. Procedures

Polymerizations were carried out under a dry argon atmosphere in a 500 mL six-neck round-bottom flask equipped with a magnetic stirrer, fitted with PTFE stopcocks and previously flamed under vacuum. The reaction volume was around 110 mL, a volume necessary to immerse properly the probes. During the polymerization process, the reactor was externally thermoregulated at a given temperature (±0.1 °C).

2.2.1. Block copolymerization

Stored in graduated tubes, the solvent was added through glass connectors to the reactor ($V = 100$ mL). When the desired temperature was reached, the MIR spectrum (1710–1550 cm^{-1}) was collected. Then the first monomer was added in the same manner ($V \approx 2$–5 mL). MIR spectrum of the solution gave the initial spectrum of the monomer (after subtraction of the absorbance due to the solvent). *sec*-Butyllithium was introduced by using a syringe, to initiate the polymerization ($V < 1$ mL). During the propagation step, MIR spectra were collected to follow the monomer consumption. At the same time, UV–visible spectra (250–650 nm) served to measure the concentration in active species.

After total consumption of the first monomer (polymerization time took ten times longer than half-polymerization time), the second monomer was introduced through a syringe ($V < 1$ mL). The cross-addition was followed by UV–visible spectroscopy at fixed wavelength (λ_{max}).

2.2.2. Statistical copolymerization

Solvent, isoprene and styrene, stored in graduated tubes, were successively added through glass connectors to the reactor. After each addition, MIR spectra were collected (1710–1550 cm^{-1}) to obtain those of isoprene and styrene (after subtraction of the absorbance due to the solvent). Then, *sec*-butyllithium was introduced using a syringe to initiate the copolymerization. Throughout the reaction, MIR spectra were taken to measure the concentrations of both monomers. Simultaneously, UV–visible spectra (250–650 nm) served to measure the concentration in active species.

2.2.3. In situ MIR spectroscopy

The polymerization reactions were followed in real time using an optical fiber probe (Remspec Inc.) equipped with a transmission head (HD 02). The mid-IR signal travels from the probe through a ZnSe window and is reflected back into the probe by a mirror surface after travelling across a short space filled by the reaction medium in which the probe is immersed. The total path length is adjustable from about 0.1 mm to about 6 mm. This probe is connected through optical fiber cables to a Tensor 27 FTIR spectrophotometer (Bruker Inc.). The signal resolution was 4 cm^{-1}. Background spectrum was taken before addition of solvent and reactants. IR spectra (64 acquisitions each) were taken every 2 min during the polymerization process. The solvent spectrum, first multiplied by its molar proportion in the polymerization mixture,

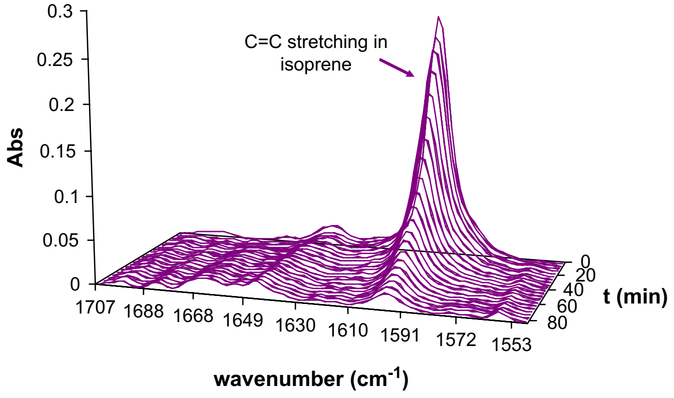

Fig. 2. Real time IR plots during the polymerization of isoprene in cyclohexane at 40 °C ($[\text{I}]_0 = 0.31$ mol L^{-1}, $[\text{PILi}] = 1.7 \times 10^{-3}$ mol L^{-1}).

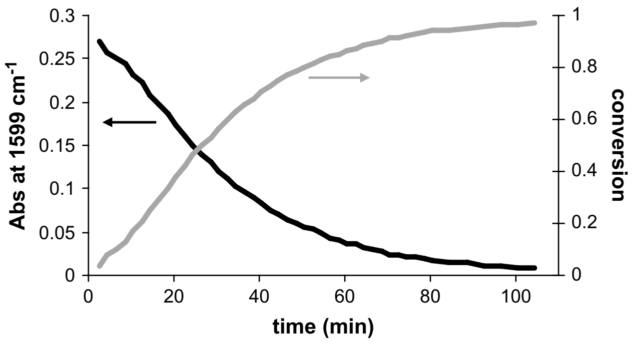

Fig. 3. IR absorbance at 1599 cm^{-1} and isoprene conversion versus time for the polymerization of isoprene in cyclohexane at 40 °C ($[\text{I}]_0 = 0.31$ mol L^{-1}, $[\text{PILi}] = 1.7 \times 10^{-3}$ mol L^{-1}).

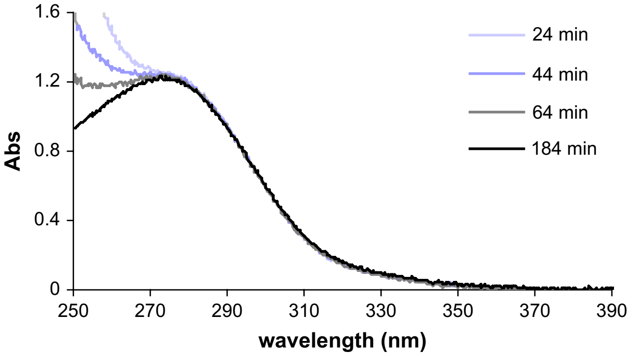

Fig. 4. Real time UV–visible plots during the polymerization of isoprene in cyclohexane at 40 °C ($[PILi] = 1.7 \times 10^{-3}$ mol L^{-1}).

was subtracted to each spectrum. Calibrations were carried out in order to demonstrate the proportionality between the monomers concentrations ($[I] < 1$ mol L^{-1}, $[S] < 0.6$ mol L^{-1}) and the intensity of 1597 cm^{-1} and 1630 cm^{-1} signals that are characteristics of the C=C stretching of isoprene and styrene, respectively.

2.2.4. *In situ UV–visible spectroscopy*

The polymerization reactions were followed in real time using a quartz immersion probe 661.302-UV (Hellma Inc., optical path: 0.1 cm) connected by optical fiber cables to a CARY 3E spectrometer (Varian Inc.).

3. Results and discussion

The rate constants of homopolymerization k_{ss} and k_{ii} and of cross-addition k_{si} and k_{is} were first determined in cyclohexane at 40 °C in order to establish a comparison with the results obtained by Worsfold – who used a high vacuum technique [13] – and thus assess the pertinence and suitability of our experimental set-up.

3.1. *I-*b*-S block copolymers*

3.1.1. *Homopropagation of isoprene*

The anionic polymerization of isoprene in cyclohexane was initiated at 40 °C using *sec*-butyllithium ($[I]_o = 0.31$ mol L^{-1}, $[sec\text{-}BuLi]_o = 1.7 \times 10^{-3}$ mol L^{-1}). Throughout the propagation step, the isoprene consumption was monitored in real time through the disappearance of the 1599 cm^{-1} band, characteristic of the C=C stretching for isoprene (Fig. 2). The Beer–Lambert law was checked at 1599 cm^{-1} for an isoprene concentration of 0.6 mol L^{-1} or below; all data abode by that law and thus absorbance could be directly converted into monomer conversion (Fig. 3). Simultaneously, the concentration in polyisoprenyllithium could be measured by UV–visible spectroscopy at $\lambda_{max} = 275$ nm ($\varepsilon = 6900$ L mol^{-1} cm^{-1} [22]). Fig. 4 exhibits a constant absorbance at 275 nm throughout polymerization, meaning that any loss in active species – if occurring – is negligible. In other words, the experimental set-up utilized here to investigate the kinetics of polymerization of isoprene, which implied the presence of IR and UV probes in the reaction medium, did not harm or even affect its "living" character. In Fig. 4, the absorbance seen at 270 nm undergoes a decrease with time, which is due to the monomer consumption.

Table 1
Rate constants k_{ii}, k_{is}, k_{ss} and k_{si} in cyclohexane at 40 °C.

k_{ii} ($L^{1/4}$ $mol^{-1/4}$ s^{-1})	k_{is} ($L^{1/4}$ $mol^{-1/4}$ s^{-1})	$r_i = k_{ii}/k_{is}$	k_{ss} ($L^{1/2}$ $mol^{-1/2}$ s^{-1})	k_{si} ($L^{1/2}$ $mol^{-1/2}$ s^{-1})	$r_s = k_{ss}/k_{si}$	Reference
3.2×10^{-3}	2.5×10^{-4}	12.8	2.4×10^{-2}	0.47	0.051	This work
3.41×10^{-3}	2.37×10^{-4}	14.4	2.29×10^{-2}	0.513	0.046	[13]

According to Worsfold and Bywater [23], polyisoprenyllithium chain ends form tetrameric aggregated species in non-polar solvents in a range of concentration of 10^{-3} mol L^{-1}. These tetrameric aggregates imply a fractional kinetic order in polyisoprenyllithium equal to ¼ [22] owing to the fact that only a small proportion of the species under unimeric form propagates (Equilibrium (1) and Reaction (2)).

$$(PILi)_4 \rightleftarrows 4PILi \tag{1}$$

$$PILi + M \rightarrow (PI)MLi \tag{2}$$

As the propagation step is a first-order kinetics with respect to the monomer concentration, the expression of the propagation rate is given by:

$$R_{ii} = \frac{d[I]}{dt} = -k_{ii}[I]\,[PILi]^{1/4} \tag{3}$$

Considering the concentration of active species constant during the polymerization process, Equation (3) can be integrated to obtain:

$$\mathrm{Ln}\frac{[I]_o}{[I]} = k_{ii}[PILi]^{1/4}t \tag{4}$$

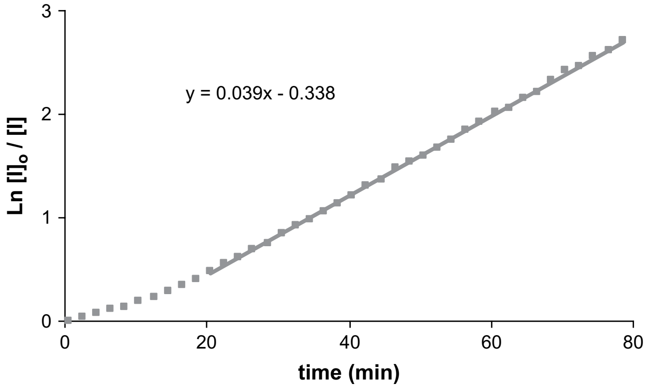

Fig. 5. First-order time–conversion plot for the polymerization of isoprene in cyclohexane at 40 °C ($[I]_o = 0.31$ mol L^{-1}, $[PILi] = 1.7 \times 10^{-3}$ mol L^{-1}).

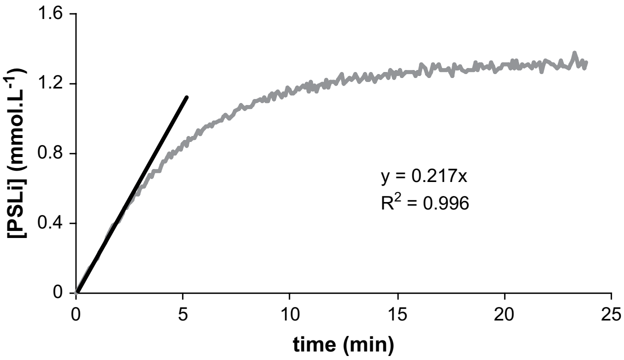

Fig. 6. PSLi formation during the cross-addition of PILi to styrene in cyclohexane at 40 °C ($[PILi]_o = 1.7 \times 10^{-3}$ mol L^{-1}, $[S]_o = 0.07$ mol L^{-1}).

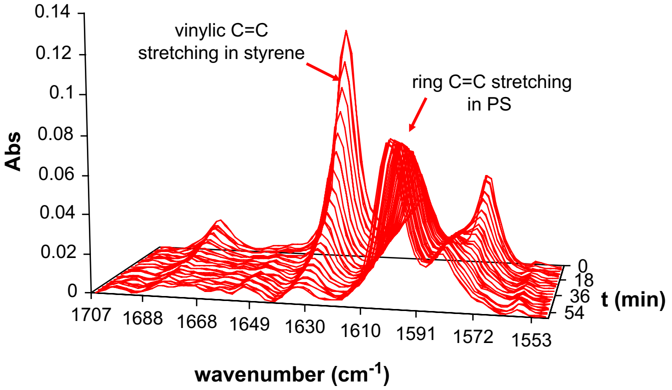

Fig. 7. Real time IR plots during the polymerization of styrene in cyclohexane at 40 °C ($[S]_o = 0.36$ mol L^{-1}, $[PSLi] = 1.2 \times 10^{-3}$ mol L^{-1}).

Thus, from the slope of the first-order time–conversion plot (Fig. 5) the rate constant k_{ii} can be determined (Table 1). It can be seen that the initial part of the curve is not linear due to the existence of an induction period that mirrors a slow initiation step in cyclohexane [24].

3.1.2. *Cross-over reaction of polyisoprenyllithium onto styrene monomer*

Upon cross-addition of PILi onto styrene under the same conditions, cyclohexane and 40 °C, the appearance of PSLi could be followed in real time by UV–visible spectroscopy at $\lambda_{max} = 328$ nm ($\varepsilon = 13{,}500$ L mol^{-1} cm^{-1} [8]). The initial rate of reaction ($R_{is,o}$) could be deduced from the initial slope of the $[PSLi] = f(t)$ curve (Fig. 6). Then, the value of the rate constant k_{is} (Table 1) was calculated using the following equation of cross-addition of PILi to styrene [13]:

$$R_{is,o} = -\left(\frac{d[PSLi]}{dt}\right)_o = k_{is}[S]_o\,[PILi]_o^{1/4} \tag{5}$$

During reaction, the formation of mixed-aggregates involving PSLi and PILi makes the kinetic results more difficult to account for [13]. That is why Equation (5) was only applied to the first moments of the cross-over reaction.

Fig. 6 also shows that the final concentration in PSLi was not equal to the initial concentration in PILi. This is due to the fact that the cross-addition of PILi to styrene is slower than the homopropagation of the latter, which was used up before all PILi could be transformed into PSLi.

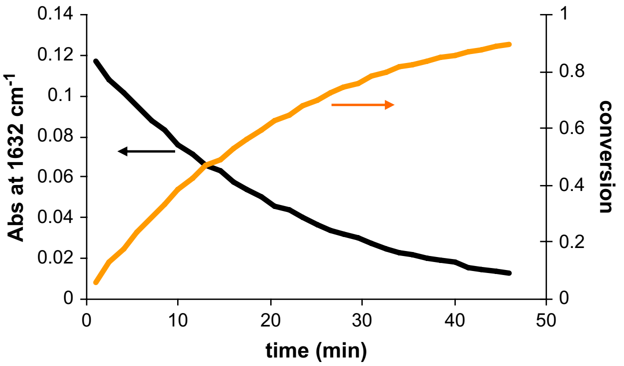

Fig. 8. IR absorbance at 1632 cm^{-1} and styrene conversion versus time for the polymerization of styrene in cyclohexane at 40 °C ($[S]_o = 0.36$ mol L^{-1}, $[PSLi] = 1.2 \times 10^{-3}$ mol L^{-1}).

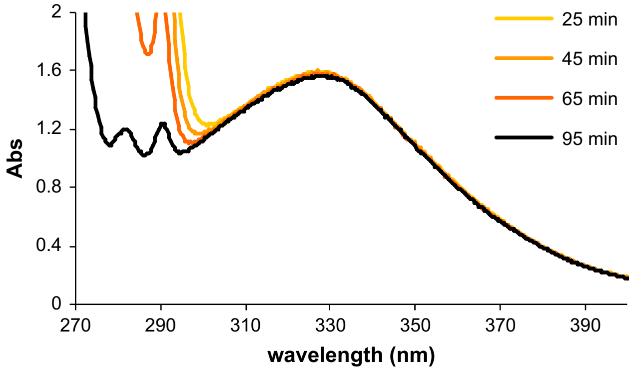

Fig. 9. Real time UV–visible plots during polymerization of styrene in cyclohexane at 40 °C ($[PSLi] = 1.2 \times 10^{-3}$ mol L^{-1}).

Knowing both propagation and cross-addition rate constants, the reactivity ratio $r_i = k_{ii}/k_{is}$ could be easily deduced: $r_i = 12.6$, which indicates that PILi prefers to add isoprene monomer rather than styrene.

3.2. *S*-b-*I block copolymers*

The kinetic procedure followed for the preparation of S-*b*-I block copolymers was quite comparable to that described for I-*b*-S. The same methodology as described above was indeed followed to determine the propagation rate constant of styrene and the rate constant of cross-addition to isoprene (k_{ss} and k_{si}) from one single experiment.

3.2.1. *Homopropagation of styrene*

During the homopolymerization of styrene initiated by *sec*-butyllithium in cyclohexane at 40 °C ($[S]_o = 0.36$ mol L^{-1}, $[PSLi] = 1.2 \times 10^{-3}$ mol L^{-1}), the monomer consumption was followed in real time through the disappearance of the 1632 cm^{-1} band that corresponds to the stretching of the vinylic C=C bond of styrene (Fig. 7). Since the Beer–Lambert law is valid ($[S] < 1.0$ mol L^{-1}), the variation of absorbance at 1632 cm^{-1} could be directly converted into conversion (Fig. 8).

Simultaneously, the concentration in active species was measured by UV–visible spectroscopy ($\lambda_{max} = 328$ nm). As evidenced by Fig. 9, the polymerization exhibits a truly “living” character with no loss of active species, the intensity of the absorbance at 328 nm remaining indeed unchanged throughout polymerization. In contrast the peak appearing at 300 nm decreased with time, indicating monomer consumption.

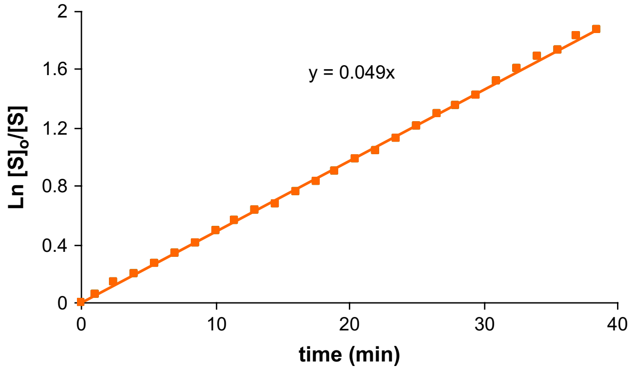

Fig. 10. First-order time–conversion plot for the polymerization of styrene in cyclohexane at 40 °C ($[S]_o = 0.36$ mol L^{-1}, $[PSLi] = 1.2 \times 10^{-3}$ mol L^{-1}).

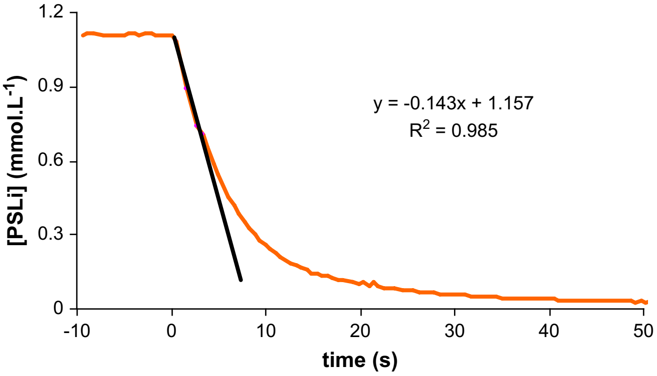

Fig. 11. PSLi consumption during cross-addition of PSLi to isoprene in cyclohexane at 40 °C ($[\mathrm{PSLi}]_o = 1.2 \times 10^{-3}$ mol L^{-1}, $[\mathrm{I}]_o = 9.1 \times 10^{-3}$ mol L^{-1}).

In non-polar solvents, polystyryllithium chain ends form dimeric aggregates [23]. As only unimeric species in equilibrium with dimeric ones propagate (Equilibrium (7) and Reaction (8)), it results a one-half kinetic order in polystyryllithium [14].

$$(\mathrm{PSLi})_2 \rightleftarrows 2\mathrm{PSLi} \tag{7}$$

$$\mathrm{PSLi} + \mathrm{M} \rightarrow (\mathrm{PS})\mathrm{MLi} \tag{8}$$

As the propagation step has a first-order kinetics with respect to the monomer concentration, the expression of the propagation rate is given by:

$$R_{ss} = \frac{d[\mathrm{S}]}{dt} = -k_{ss}[\mathrm{S}]\ [\mathrm{PSLi}]^{1/2} \tag{9}$$

As the concentration of active species is constant throughout polymerization, the integration of Equation (9) gives:

$$\mathrm{Ln}\frac{[\mathrm{S}]_o}{[\mathrm{S}]} = k_{ss}[\mathrm{PSLi}]^{1/2}t \tag{10}$$

Thus, from the slope of the straight line describing the variation of Ln $[\mathrm{S}]_o/[\mathrm{S}]$ versus time (Fig. 10) the rate constant k_{ss} could be easily deduced (Table 1).

3.2.2. *Cross-over reaction of polystyryllithium onto isoprene*

Upon addition of isoprene to living PSLi in cyclohexane at 40 °C, the absorbance of the latter species decreased which could be followed in real time by UV–visible spectroscopy set at 328 nm. The initial rate of reaction was drawn from the initial slope of the $[\mathrm{PSLi}] = f(t)$ curve (Fig. 11). Then, the value of the rate constant k_{si} was determined by using the following kinetic equation of the reaction:

$$R_{si,o} = \left(\frac{d[\mathrm{PSLi}]}{dt}\right)_o = -k_{si}[\mathrm{I}]_o\ [\mathrm{PSLi}]_o^{1/2} \tag{11}$$

As stressed previously, this kinetic equation of cross-addition is valid only as long as the presence of cross-aggregates is negligible.

The reactivity ratio $r_s = k_{ss}/k_{si}$ determined is equal to 0.051 thus indicating the preference of PSLi for isoprene rather than styrene.

The rate constants (k_{ss}, k_{ii}, k_{si} and k_{is}) determined with the help of *in situ* MIR and UV–visible spectroscopies appear to be in good agreement with the values obtained by Worsfold [13] under similar conditions (cyclohexane, 40 °C) (Table 1). Our experimental set-up is thus well suited to monitor the kinetics of anionic polymerization with its constraints of concentration and rate ($[\mathrm{C}^*] \approx 1 \times 10^{-3}$ mol L^{-1}, $t_{1/2} < 1$ h). A fast and accurate measurement of propagation and cross-addition rate constants could indeed be made from one single experiment. Owing to experimental conditions used, the accuracy of measurement is estimated to be around 90%.

3.3. *Effect of the nature of the non-polar solvent*

After demonstrating the suitability of our experimental set-up under conditions reported in the literature, we then investigated the solvent effect on the reactivity of styrene and isoprene when (co)polymerized. To this end, the propagation and cross-reaction rate constants (k_{ss}, k_{si}, k_{ii} and k_{is}) were determined at 30 °C in 3 aromatic solvents: benzene, toluene and ethylbenzene. Indeed, the values of these rate constants are available in the literature for cyclohexane[18] and for benzene[23] but not for toluene and ethylbenzene which are solvents of reportedly lesser toxicity and thus of interest to industry.

The data generated are shown in Tables 2 and 3, the k_{ss} value measured in ethylbenzene being the smallest. A little but significant difference is observed between the k_{ss} value measured in toluene and in ethylbenzene indicating that, at 30 °C, the rate of propagation is slightly faster in toluene than in ethylbenzene ($k_{ss,tol} = 1.6 \times 10^{-2}$ L$^{1/2}$ mol$^{-1/2}$ s^{-1} and $k_{ss,eth} = 1.1 \times 10^{-2}$ L$^{1/2}$ mol$^{-1/2}$ s^{-1}), the value in benzene being intermediate.

This difference is illustrated in the conversion–time plots of Fig. 12. Under equivalent conditions ($T = 30$ °C, $[\mathrm{PSLi}] = 1.2 \times 10^{-3}$ mol L^{-1}), the half-polymerization time is higher by 7 min in ethylbenzene ($t_{1/2} = 28$ min) than in toluene ($t_{1/2} = 21$ min). Such kinetic data are essential for the optimization of the polymerization time since both solvents – toluene and ethylbenzene – are prone to transfer, especially at higher temperatures, which then requires to be minimized.

3.4. *Effect of temperature*

The effect of temperature on the rate constant of propagation of styrene k_{ss} was investigated in toluene, ethylbenzene and benzene from 20 to 40 °C ($[\mathrm{C}^*] \approx 10^{-3}$ mol L^{-1}), in order to determine the energy of activation in these solvents. The rate of propagation for styrene at 20 and 40 °C was observed to increase in the following order: ethylbenzene < benzene < toluene, as reported above. The corresponding activation energies were determined using Arrhenius plots (Fig. 13). Within the experimental error associated with

Table 2
Rate constants k_{ii} and k_{is} at 30 °C in benzene, toluene and ethylbenzene.

Solvent	$[\mathrm{I}]_o$ (mol L^{-1})	[PILi][a] (mol L^{-1})	k_{ii} [PILi]$^{1/4}$[b] (s^{-1})	k_{ii} (L$^{1/4}$ mol$^{-1/4}$ s^{-1})	$[\mathrm{S}]_o$ (mol L^{-1})	$R_{(is)o}$[c] (mol L^{-1} s^{-1})	k_{is} (L$^{1/4}$ mol$^{-1/4}$ s^{-1})	$r_i = k_{ii}/k_{is}$
Benzene	0.30	1.30×10^{-3}	2.9×10^{-4}	1.5×10^{-3}	0.09	2.7×10^{-6}	1.7×10^{-4}	9.2
Toluene	0.28	1.10×10^{-3}	2.5×10^{-4}	1.4×10^{-3}	0.08	2.3×10^{-6}	1.6×10^{-4}	8.8
Ethylbenzene	0.36	1.05×10^{-3}	2.6×10^{-4}	1.4×10^{-3}	0.08	2.4×10^{-6}	1.7×10^{-4}	8.4

[a] Measured by UV–visible at 280 nm ($\varepsilon = 6900$ L mol^{-1} cm^{-1}).
[b] Slope of the first-order time–conversion plot.
[c] Measured by UV–visible at 335 nm ($\varepsilon = 13{,}000$ L mol^{-1} cm^{-1}).

Table 3
Rate constants k_{ss} and k_{si} at 30 °C in benzene, toluene and ethylbenzene.

Solvent	$[S]_o$ (mol L^{-1})	[PSLi][a] (mol L^{-1})	k_{ss} [PSLi]$^{1/2}$[b] (s^{-1})	k_{ss} (L$^{1/2}$ mol$^{-1/2}$ s^{-1})	$[I]_o$ (mol L^{-1})	$R_{(si)o}$[a] (mol L^{-1} s^{-1})	k_{si} (L$^{1/2}$ mol$^{-1/2}$ s^{-1})	$r_s = k_{ss}/k_{si}$
Benzene	0.30	1.15×10^{-3}	4.75×10^{-4}	1.4×10^{-2}	0.9×10^{-2}	1.1×10^{-6}	0.36	0.040
Toluene	0.32	1.25×10^{-3}	5.65×10^{-4}	1.6×10^{-2}	1.0×10^{-2}	1.3×10^{-6}	0.37	0.044
Ethylbenzene	0.36	1.30×10^{-3}	4.15×10^{-4}	1.1×10^{-2}	1.0×10^{-2}	1.3×10^{-4}	0.38	0.031

[a] Measured by UV–visible at 335 nm ($\varepsilon = 13{,}000$ L mol^{-1} cm^{-1}).
[b] Slope of the first-order time–conversion plot.

the measurement of k_{ss}, the values of 60, 62 and 63 kJ mol^{-1} were found for E_a in toluene, benzene and ethylbenzene, respectively; the comparison with the value obtained by Worsfold and Bywater in benzene: $E_a = 60$ kJ mol^{-1} [14] thus results in an excellent agreement.

The effect of temperature on the kinetics of block polymerization of styrene and isoprene was then examined from 12 to 40 °C in benzene. The activation energies of each step of the block copolymerization process were measured using Arrhenius plots for the following rate constants k_{ss}, k_{si}, k_{ii} and k_{is} (Fig. 14). The activation energy for homopropagation of isoprene is 75 kJ mol^{-1} and those of cross-additions of PILi to styrene and of PSLi to isoprene are 64 and 59 kJ mol^{-1}, respectively.

3.5. Statistical copolymerization of styrene and isoprene

The copolymerization of styrene and isoprene was initiated by *sec*-butyllithium in benzene at 30 °C and followed by MIR and UV–visible spectroscopies ($[S]_o/[I]_o = 50/50$). On the one hand, styrene and isoprene conversions could be monitored using the 1597 cm^{-1} and 1630 cm^{-1} stretching bands that are characteristic of vinylic C=C in isoprene and styrene, respectively (Figs. 15 and 16). On the other hand, the variation of the PSLi concentration could be followed by UV spectroscopy at 332 nm (Fig. 16).

The copolymerization of styrene and isoprene can be described through 4 reactions (12–15). In the early stages of the copolymerization, no measurable UV signal attributable to PSLi species could be detected. This is due to a slow reaction of styrene with PILi ($k_{is} < k_{ii}$) compared to isoprene and to a very fast reaction of isoprene with any PSLi formed ($k_{si} > k_{ss}$) compared to styrene. In the early stages of the process (Fig. 16) the probability of formation of PSLi is negligible and thus the consumption of isoprene is favoured. As the concentration of isoprene decreases with conversion, the rate of incorporation of styrene into the copolymer chains increases. In the later stages of the reaction, when isoprene has been largely used up, the chain grows by consuming almost exclusively styrene.

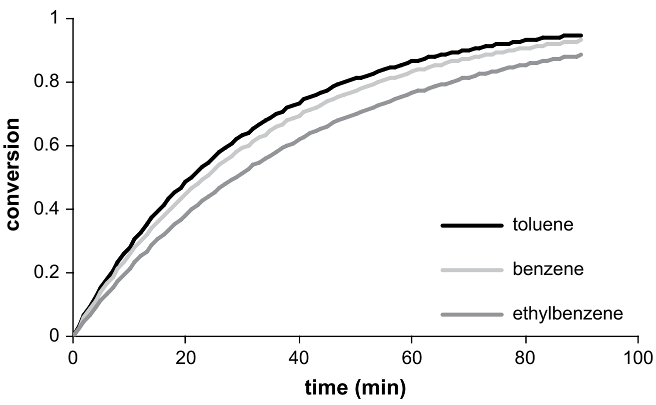

Fig. 12. Styrene time–conversion plots in toluene, benzene and ethylbenzene ($[\mathrm{PSLi}] = 1.2 \times 10^{-3}$ mol L^{-1}, $T = 30$ °C).

$$(\mathrm{PILi})_4 \rightleftarrows 4\mathrm{PILi}$$

$$\mathrm{PILi} + \mathrm{I} \rightarrow (\mathrm{PI})\mathrm{ILi} \tag{12}$$

$$\mathrm{PILi} + \mathrm{S} \rightarrow (\mathrm{PI})\mathrm{SLi} \tag{13}$$

$$(\mathrm{PSLi})_2 \rightleftarrows 2\mathrm{PSLi}$$

$$\mathrm{PSLi} + \mathrm{S} \rightarrow (\mathrm{PS})\mathrm{SLi} \tag{14}$$

$$\mathrm{PSLi} + \mathrm{I} \rightarrow (\mathrm{PS})\mathrm{ILi} \tag{15}$$

The kinetic equations describing the variation of the concentration of monomers and of active species during the copolymerization can be written for the reactions (12–15):

$$\frac{d[\mathrm{I}]}{dt} = -k_{ii}[\mathrm{I}]\,[\mathrm{PILi}]^{1/4} - k_{si}[\mathrm{I}]\,[\mathrm{PSLi}]^{1/2} \tag{16}$$

$$\frac{d[\mathrm{S}]}{dt} = -k_{ss}[\mathrm{S}]\,[\mathrm{PSLi}]^{1/2} - k_{is}[\mathrm{S}]\,[\mathrm{PILi}]^{1/4} \tag{17}$$

$$\frac{d[\mathrm{PSLi}]}{dt} = -k_{si}[\mathrm{I}]\,[\mathrm{PSLi}]^{1/2} + k_{is}[\mathrm{S}]\,[\mathrm{PILi}]^{1/4} \tag{18}$$

$$\frac{d[\mathrm{PILi}]}{dt} = -k_{is}[\mathrm{S}]\,[\mathrm{PILi}]^{1/4} + k_{si}[\mathrm{I}]\,[\mathrm{PSLi}]^{1/2} \tag{19}$$

According to Fig. 16, [PSLi] can be considered as constant during the early stages of the process. Thus,

$$\frac{d[\mathrm{PSLi}]}{dt} = 0$$

corresponds to a steady-state situation.

From equation (18):

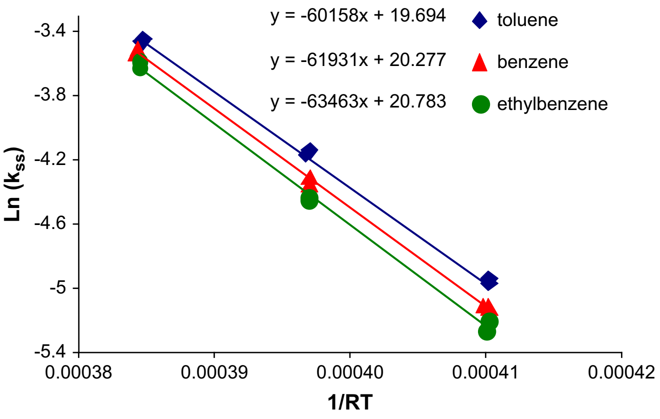

Fig. 13. Effect of temperature on rate constant k_{ss} in toluene, benzene and ethylbenzene.

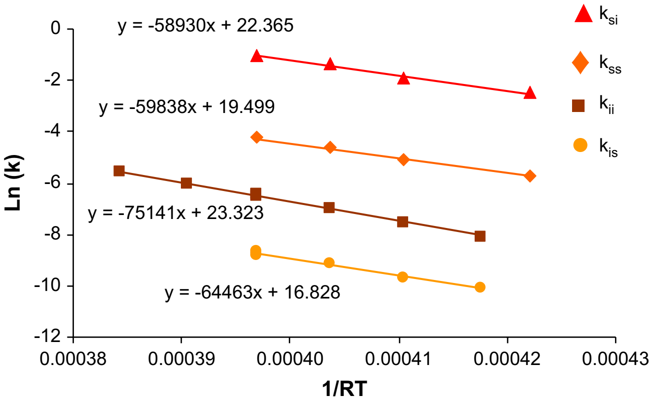

Fig. 14. Effect of temperature on rate constants k_{si}, k_{ss}, k_{ii} and k_{is} in benzene.

$$k_{si}[\mathrm{I}]\ [\mathrm{PSLi}]^{1/2} = k_{is}[\mathrm{S}]\ [\mathrm{PILi}]^{1/4}.$$

Then, taking the ratio of Equation (16) to Equation (17) yielded Equation (20) commonly called “Mayo–Lewis Equation” and mostly used in radical copolymerization.

$$\frac{\mathrm{d}[\mathrm{I}]}{\mathrm{d}[\mathrm{S}]} = \frac{[\mathrm{I}]\ (r_i[\mathrm{I}] + [\mathrm{S}])}{[\mathrm{S}]\ ([\mathrm{I}] + r_s[\mathrm{S}])} \quad \text{with } r_i = \frac{k_{ii}}{k_{is}} \text{ and } r_s = \frac{k_{ss}}{k_{si}} \tag{20}$$

Both styrene and isoprene concentrations were measured in real time by MIR spectroscopy. From these data the Mayo–Lewis equation could be solved by using a least square method:

$r_i = 10.7$ and $r_s = 0.047$ in benzene at 30 °C.

These reactivity ratios are close to those obtained from the block copolymerization study ($r_i = 9.2$ and $r_s = 0.040$). In other words, the reactivity ratios resulting from the copolymerization of styrene and isoprene can be measured accurately from one single experiment involving simultaneously MIR and UV–visible spectroscopies. If MIR spectroscopy has already been utilized for the determination of reactivity ratios in anionic copolymerization [11], its combination with UV–visible spectroscopy is an irreplaceable means to confirm the “living” character of the copolymerization.

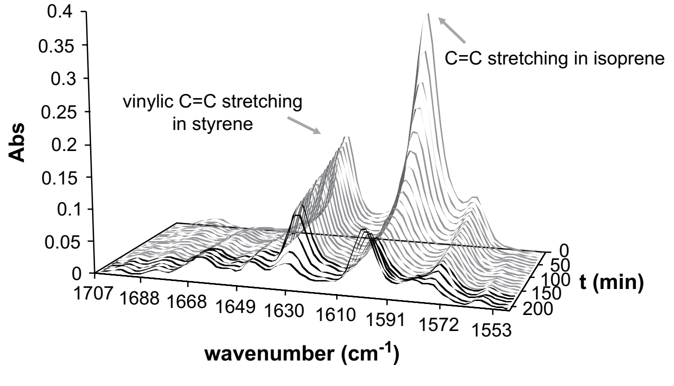

Fig. 15. Real time IR plots during copolymerization of styrene and isoprene in benzene at 30 °C ($[\mathrm{S}]_o = [\mathrm{I}]_o = 0.42\ \mathrm{mol\ L^{-1}}$, $[\mathrm{C}^*] = 1.3 \times 10^{-3}\ \mathrm{mol\ L^{-1}}$).

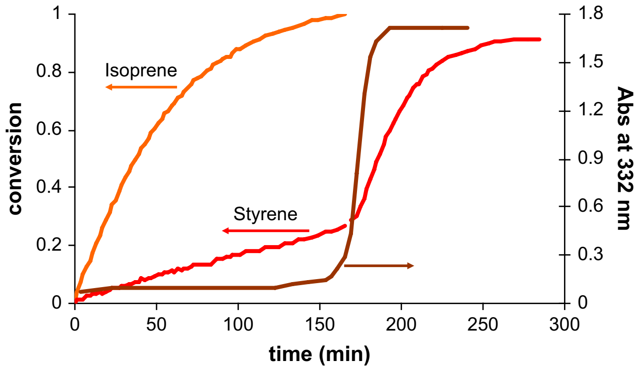

Fig. 16. Monomers time–conversion plots and UV absorbance at 332 nm versus time for the copolymerization of styrene and isoprene in benzene at 30 °C ($[\mathrm{S}]_o = [\mathrm{I}]_o = 0.42\ \mathrm{mol\ L^{-1}}$, $[\mathrm{C}^*] = 1.3 \times 10^{-3}\ \mathrm{mol\ L^{-1}}$).

4. Conclusion

The combination of *in situ* MIR and UV–visible spectroscopies was shown to be perfectly suited to the simultaneous monitoring of the monomer consumption and chain end concentrations in the anionic copolymerization of styrene and isoprene. A fast and accurate determination of the rate constants of propagation and cross-addition (k_{ss}, k_{si}, k_{is}, k_{ii}) could be achieved, the values obtained being in good agreement with literature data. From one single copolymerization experiment, the reactivity ratios (r_s, r_i) of the anionic copolymerization of styrene and isoprene could also be reliably obtained using this analytical tool.

The investigation of the solvent effect on kinetic parameters showed that the only reaction to depend on the type of apolar solvent used is the propagation step of styrene. In the same conditions (temperature and chain end concentration), the half-polymerization time of styrene is indeed around 25% lower in toluene than in ethylbenzene.

References

[1] Hsieh HL, Quirk RP. Anionic polymerization: principles and practical applications. New York: M. Dekker; 1996.
[2] Szwarc M. Adv Polym Sci 1983;49:1.
[3] Szwarc M, VanBeylen M. Ionic polymerization and living polymers. 1993.
[4] VanBeylen M, Bywater S, Smets G, Szwarc M, Worsfold DJ. Adv Polym Sci 1988;86:87.
[5] Hsieh HL. J Polym Sci Part A 1965;3:173.
[6] Morton M, Bostick EE, Livigni R, Fetters LJ. J Polym Sci Part A 1963;1:1735.
[7] Auguste S, Edwards HGM, Johnson AF, Meszena ZG, Nicol P. Polymer 1996;37:3665.
[8] Johnson AF, Worsfold DJ. J Polym Sci Part A 1965;3:449.
[9] Long TE, Liu HY, Schell BA, Teegarden DM, Uerz DS. Macromolecules 1993;26:6237.
[10] Ohlinger R. Makromol Chem 1980;181:1935.
[11] Williamson DT, Buchanan TD, Elkins CL, Long TE. Macromolecules 2004;37:4505.
[12] Williamson DT, Elman JF, Madison PH, Pasquale AJ, Long TE. Macromolecules 2001;34:2108.
[13] Worsfold DJ. J Polym Sci Part A-1 1967;5:2783.
[14] Worsfold DJ, Bywater S. Can J Chem 1960;38:1891.
[15] Michel AJ, Puskas JE, Brister LB. Macromolecules 2000;33:3518.
[16] Puskas JE, Chan P, McAuley KB, Kaszas G, Shaikh S. Macromol Symp 2006;240:18.
[17] Puskas JE, Lanzendörfer MG, Pattern WE. Polym Bull 1998;40:55.
[18] Puskas JE, Shaikh S. Macromol Symp 2004;215:231.
[19] Storey RF, Donnalley AB, Maggio TL. Macromolecules 1998;31:1523.
[20] Szwarc M. Carbanions, living polymers and electron transfer processes. New York: Interscience; 1968.
[21] Suffert J. J Org Chem 1989;54:509.
[22] Worsfold DJ, Bywater S. Can J Chem 1964;42:2884.
[23] Worsfold DJ, Bywater S. Macromolecules 1972;5:393.
[24] Bywater S, Worsfold DJ. J Organomet Chem 1967;10:1.